

# High Resolution Optical Doppler Tomography for *in vivo* Blood Flow Dynamics with Pharmacological Intervention

Cheng-Jen Chang\*    Zhong-Ping Chen<sup>1</sup>

*Department of Plastic and Reconstructive Surgery, Chang Gung Memorial Hospital, Taipei, Taiwan, 105, ROC*

<sup>1</sup>*Beckman Laser Institute, University of California Irvine, Irvine, CA, U.S.A.*

Received 2 July 2003; Accepted 10 Aug 2003

---

## Abstract

High spatial resolution noninvasive techniques for *in vivo* blood flow imaging are currently not available as a diagnostic tool in clinical medicine. Such techniques could have a significant impact for biomedical research and clinical diagnosis. The rationale for using Optical Doppler Tomography (ODT) to characterize the underlying microvasculature is that the technique will be able to probe user-specified discrete spatial locations with high spatial resolution. The objective of our research is to use a noninvasive tomographic imaging technique with high spatial resolution (2-15  $\mu\text{m}$ ) to characterize and monitor fluid flow and microvasculature in highly scattered biological tissues at user-specified discrete locations. ODT combines Laser Doppler Flowmetry (LDF) with optical coherence tomography (OCT) to obtain high-resolution tomographic velocity and structural images of static and moving constituents biological tissue with high light scattering properties. ODT demonstrates the ability to simultaneously record structure and velocity in images. We present ODT images of structure and velocity using *in vivo* blood flow in the Chick Chorioallantoic Membrane (CAM). ODT images were also recorded before and after topical application of nitroglycerin. ODT images of *in vivo* CAM blood flow demonstrate that the magnitude of blood flow velocity at the center of the vein is maximal and that it decreases monotonically towards the peripheral wall. The arterial wall can be clearly identified by its dilatation after the application of nitroglycerin. Peak blood flow velocity at the center of the artery increased from 3000 to 4000  $\mu\text{m/s}$  after nitroglycerine application. Dilatation of the vein due to nitroglycerine is observed in both the structure and velocity at the center of the vein. It decreased from 2000 to 1000  $\mu\text{m/s}$  after nitroglycerin application. In conclusion, in our *in vivo* studies on CAM model vasculatures, the application of ODT to characterize and image blood flow with high spatial resolution at discrete user-specified locations in biological tissues with high light scattering properties is feasible.

**Keywords:** Optical doppler tomography, Laser doppler flowmetry, Optical coherence tomography, Microvasculature

---

## Introduction

Noninvasive techniques for imaging *in vivo* blood flow are of great value for biomedical research and clinical diagnostics [1]. The ideal microvascular imaging technique must fulfill several requirements: a) probe the underlying microcirculation at a user-specified depth in both superficial and deep layers; b) distinguish arterial from venous flow; c) detect blood flow changes rapidly; and d) be safe, noninvasive, reliable, and reproducible. Numerous approaches have been investigated including angiography, electromagnetic flowmetry, and magnetic resonance imaging (MRI)[2]. All of these techniques have shown limited utility for tomographic imaging of the microcirculation. More recent approaches have incorporated the Doppler effect [3, 4].

Doppler ultrasound imaging technique uses the principle

that the frequency of ultrasonic waves are backscattered by moving red blood cells (RBC) [3]. In addition to being noninvasive, the chief advantage of the Doppler ultrasound technique is its ability to record images of the heart and large diameter blood vessels (e.g., >1 mm). However, the relatively long acoustic wavelengths required for deep tissue penetration limit spatial resolution to approximately 200  $\mu\text{m}$ .

Laser Doppler Flowmetry (LDF) was first described in the 1960's by Yeh and Cummins [5]. However, it was not until 1972 that the first blood flow measurement using LDF was demonstrated [6]. LDF uses a single optical frequency which provides a highly coherent light incidence entering the tissue. A second fiber collects the backscattered light; two variables are recorded from this information. One is the velocity of the blood flow, which detected by measuring the movement of the RBC. The other interpretation recognizes static constituents of the tissue. Light scattered exclusively by static constituents has no frequency change. Detection of the Doppler shift is

---

\* Corresponding author: Cheng-Jen Chang  
Tel: +886-2-27135211 ext.3502; Fax: +886-2-25140600  
E-mail: chengjen@adm.cgmh.org.tw

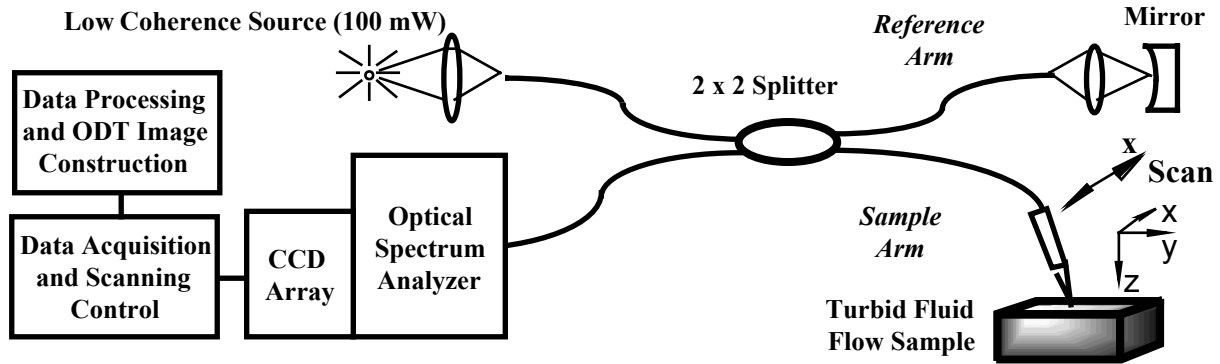


Figure 1. Schematic diagram of the proposed spectral ODT instrument.

founded on the heterodyne beating principle: shifted and non-shifted backscattered light amplitudes are mixed on the surface of a photoreceiver to produce low frequency ( $< 10$  kHz) intensity fluctuations. The power spectrum of such fluctuations is a complex function of RBC velocity distribution and concentration in the microvasculature [4]. Unfortunately, because the signal of LDF based on is multiple scattered light with a corresponding large variance in optical path lengths through the tissue, spatial resolution is poor ( $> 250$   $\mu\text{m}$ ) and information relevant to blood flow at a discrete location is lost.

Spatial resolution of conventional LDF can be improved by using coherence gating. Optical Doppler Tomography (ODT) [7-8], combines LDF with optical coherence tomography (OCT) [9-12] to obtain high resolution tomographic images of static and moving constituents in biological tissues with high scattering properties. Such localization is possible because the detected ODT interference fringe intensity gives an accurate discrimination of the optical path length of Doppler shifted and backscattered light to within the source coherence length. Furthermore, in contrast the ODT signal from moving RBC is almost entirely due to the Doppler shifted backscattered light. As a result, signal to noise ratios are substantially higher. Raster scanning the target fiber probe allows construction of a three-dimensional tomographic map of the underlying microcirculation. It is obvious that a method that can probe blood flow at discrete user-specified locations in biological tissues with high light scattering properties would have decided advantages over existing methodologies. The purposes of this study are to (1) investigate the effects of multiple light scattering and coherence gating on ODT images by simulating light absorption and scattering in turbid fluid flow media using Monte Carlo methods, (2) develop a high speed ODT instrument for tomographic imaging of *in vivo* blood flow in biological tissues with high light scattering properties.

## Materials and Methods

The proposed research is directed toward the development of a high speed ODT system for imaging *in vivo* blood flow. To this end, we propose three principal efforts. First, an ODT system based on spectral interferometry will be

designed and constructed. Second, a mathematical model that includes light scattering and absorption in RBC and surrounding tissues will be developed. Monte Carlo methods will be used to simulate multiple scattering and coherence gating to gain insight into the ODT imaging process. Third, a series of experiments to image *in vitro* blood flow will be carried out using the high speed ODT system.

### Design and Development of a High Speed ODT System Based on Spectral Interferometry

Our current prototype ODT instrument acquires data for each pixel serially by a sequential two-dimensional scan, which limits imaging speed. Image acquisition time for our prototype device is given by  $T = N_x N_z \Delta t_p$ , where  $N_x$  and  $N_z$  are the number of pixels in the lateral and depth dimensions, and  $\Delta t_p$  is the pixel acquisition time. Inasmuch as detection of the Doppler shift requires sampling the interference fringe intensity over at least one oscillation cycle, pixel acquisition time varies inversely with  $\Delta f_D$  (i.e.,  $\Delta t_p \approx 1/\Delta f_D$ ). Given a minimum detectable Doppler shift ( $\Delta f_D(\text{min})$ ), ODT velocity resolution ( $v_{\text{ODT}(\text{min})}$ ) is:

$$v_{\text{ODT}(\text{min})} = \frac{\Delta f_D(\text{min}) \lambda_0}{2n \cos(\theta)} \quad (1)$$

Thus, pixel acquisition time is limited not only by detection sensitivity, but also by velocity resolution. For  $v_{\text{ODT}(\text{min})} = 100$   $\mu\text{m/s}$  and  $\theta = 70^\circ$ ,  $\Delta f_D(\text{min}) = 112$  Hz or  $\Delta t_p = 9$  ms. Therefore, to achieve velocity resolution of 100  $\mu\text{m/s}$ , minimum pixel acquisition time is approximately 9 ms. In the two-dimensional scanning approach, an ODT image of 100 x 100 pixels requires a minimum acquisition time of 90 s. Imaging speed in our prototype instrument is limited because temporal interference fringe intensity data used to construct ODT structural and velocity images is acquired serially. For real-time imaging of static and moving constituents in a turbid sample, we propose to develop a high speed ODT system (Fig. 1) based on spectral interferometry, which acquires data for ODT structural and velocity images in parallel by using an optical spectrum analyzer at the interferometer output to measure time variation of spectral interference fringe intensity ( $P_{\text{ODT}}(v, t)$ ).

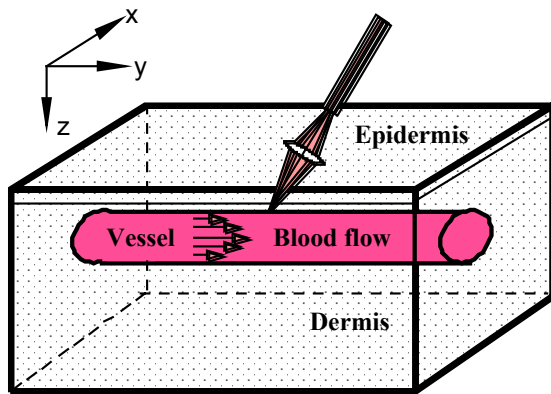


Figure 2. Physical model for Monte Carlo simulation

Optical spectral interferometry has been widely used for ranging and structural imaging [10, 13-16]. In spectral interferometry, modulation of the interference fringe intensity in the spectral domain ( $P(\nu)$ ) is used to determine the locations of all light scattering objects along the beam propagation direction. It has been shown that spectral interferometry is equivalent to coherence gating, and the signals analyzed from the complex representations of spectral ( $P(\nu)$ ) and temporal ( $\Gamma(\tau)$ ) interference fringe intensity are Fourier transform pairs [10, 16]. Measurement of  $P(\nu)$  can be used to determine  $\Gamma(\tau)$ , where  $\tau$  is related to the path length delay ( $\Delta = c\tau$ ) between light in the sample and reference arms.

Spectral ODT measures the time variation of spectral interference fringe intensity ( $P_{\text{ODT}}(\nu, t)$ ). The positions of the light scattering constituents along the beam propagation axes can be determined by an inverse Fourier transformation of the optical spectrum. The velocity of the moving particles can be determined from the oscillation frequency of the optical spectrum in the time domain. Thus, for each lateral position of the sample probe, measurement of ( $P_{\text{ODT}}(\nu, t)$ ) by an optical spectrum analyzer allows parallel acquisition of position and velocity information over  $N_z$  pixels. Because the entire spectrum of interference fringe intensity is acquired simultaneously with a detector array, image acquisition time is reduced to  $T = N_x \Delta t_p$  using spectral ODT. An ODT image of 100 lateral pixels with a velocity resolution of 100  $\mu\text{m/s}$  can be acquired in less than a second. Thus, spectral ODT allows a two-dimensional image to be acquired with one lateral scan, which reduces image acquisition time by a factor of  $N_z$  as compared to our current prototype ODT system. Because no mechanical movement is necessary to probe deeper positions when using an optical spectrum analyzer, measurement of the time variation of spectral interference fringe intensity allows rapid imaging of static and moving constituents in the turbid fluid flow sample. The proposed spectral ODT instrument consists of a fiber optic Michelson interferometer similar to our prototype instrument except that a high power low coherence source is required. A spectrum analyzer with a fast detector array will be used to acquire the time variation of spectral interference fringe intensity. Important electro-optic components for the development of spectral ODT include a

high power low coherence source and an optical spectrum analyzer with a high speed CCD detector array.

#### **Investigate the Effects of Multiple Light Scattering by Monte Carlo Simulation**

Application of ODT for *in vivo* imaging of blood flow requires an understanding of light propagation in a medium of moving RBC buried in tissues which scatter light. Although our preliminary results clearly demonstrate that *in vivo* blood flow can be imaged by ODT, the effects of many factors, such as flow velocity, blood concentration, vessel diameter, tissue scattering parameters, and detector configuration on the flow image have not been investigated. An example is the effect of multiple tissues which scatter light, which could affect Doppler flow velocity in the ODT images. Monte Carlo simulation is a versatile and often-used tool in tissue optics, where inhomogeneities and stochastic absorption and scattering parameters confuse the analysis of photon propagation in the tissue. The Monte Carlo method has been applied to simulate conventional laser Doppler velocimetry for blood perfusion measurements [17-18]. However, the effect of coherence gating on ODT has not been investigated. Our aim is to use the Monte Carlo method to simulate light scattering and coherence gating and to investigate the effect of multiple scattering and other factors on the ODT image.

The physical model comprises a blood vessel surrounded by a medium with light scattering potential (Fig. 2), which consists of epidermal and dermal layers for skin, and intralipid for *in vivo* studies. A parabolic velocity profile is assumed for blood flow in small vessels. The simulation can be divided into two components: generation of photon histories and detection with coherence gating.

To generate photon histories, individual paths of photons from a focused Gaussian beam propagating through the light scattering medium are traced. The distance between interaction points is determined by sampling an exponential probability distribution of scattering lengths. The polar scattering angle ( $\alpha$ ) is determined by the Henyey-Greenstein or a similar function [17-18]. If a photon is scattered by a moving RBC, the Doppler shift is recorded. Photons are followed until they exit the top surface or the path length exceeds a preset maximum value. Total photon path length, scattering positions, Doppler shift, and the position and angle of the exit photon through the top surface are obtained from the photon histories.

The detector component of the mode consists of a numerical aperture and coherence length gating. This component will be designed to allow investigation of different detector configurations using a single simulation. Only backscattered photons that exit from the light scattering medium within the cone, defined by the numerical aperture of the detector, will be registered. Among these, only photons with the path length matching the reference arm, within the coherence length of the light source, will produce interference fringes. A number of important statistical parameters, such as the total number of photons detected with and without Doppler frequency shift, the mean value of the frequency shift, the frequency spectrum, and the point spread function can be obtained. With a realistic light propagation model, questions

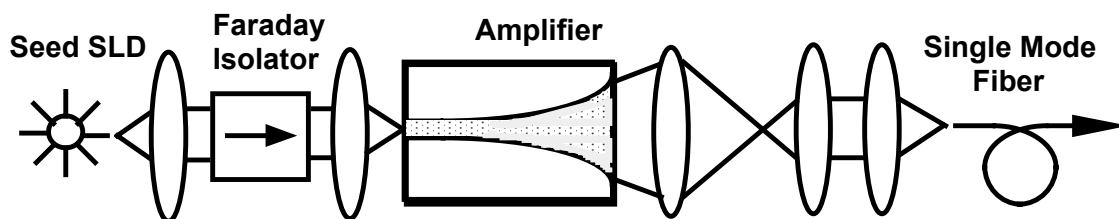


Figure 3. Optical layout of the proposed high power partially coherent source.

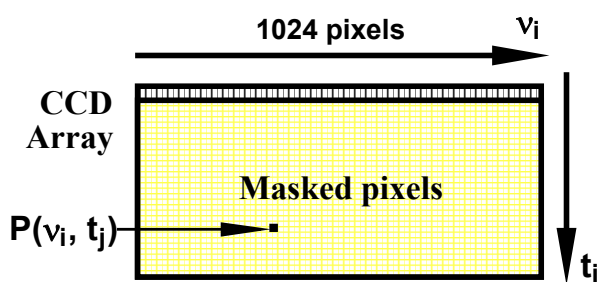


Figure 4. High speed spectral CCD

that are difficult to address experimentally, such as importance of multiple light scattering effects, various detector configurations, and changes in source coherence length, will be formulated and answered by simulation studies. Valuable information will be obtained by comparing the power spectrum at each pixel in the experimental images, with the simulated distribution of Doppler shifts, for the corresponding pixel.

Two-dimensional simulations will allow direct comparison with experimental images. Because the incidence of photons being backscattered is very small, strategies that increase the efficiency of the simulation, such as methods proposed by Stern [17] and Schmitt [19] will be implemented. Results from the simulation will also be used to optimize the design and development of the ODT instrument and signal processing.

#### Development of a High Power Low Coherence Source

Because of the parallel nature of the data acquisition process in spectral interferometry, a high power low coherence source is required to achieve adequate signal to noise ratio (SNR) for imaging *in vivo* blood flow. We propose to develop a high power low coherence light source using a p-n diode single-pass semiconductor optical amplifier (SDL, Inc.) to generate broadband amplified spontaneous emission centered at  $\nu_0 = 350$  THz ( $\lambda_0=850$  nm). The p-n diode is a single GaAs quantum well in an AlGaAs heterostructure with antireflection coatings at both ends. Optical power exceeding 200 mW coupled into a single mode fiber has been demonstrated by Goldberg *et al* using a similar source [20]. Collimated seed light emitted by a SLD is coupled into the input facet ( $4 \mu\text{m}$ ) of the optical amplifier (Fig. 3). A Faraday isolator is used to eliminate the reflected light from the optical amplifier coupling back into the SLD. Emission from the output end of the optical amplifier is collimated and

coupled into a single mode fiber. In comparison to alternative high power partially coherent sources (e.g., femtosecond lasers), the smooth noise-free power spectral density profile of the proposed source is well suited for ODT.

#### Development of the Optical Spectrum Analyzer with a High Speed Detector Array

Measurement of spectral interference fringe intensity for imaging *in vivo* blood flow in light scattering biological tissues requires a spectrum analyzer with a high speed linear detector array. The required number of pixels in the array is determined by the resolution ( $\Delta\nu$ ) of the optical spectrum analyzer, and is directly related to the maximum depth ( $\Delta_{\text{max}}$ ) that may be interpreted in the turbid sample,

$$\Delta_{\text{max}} = \frac{1}{4n} \frac{c}{\Delta\nu} = \frac{1}{4n} \frac{\lambda^2}{\Delta\lambda} \quad (2)$$

$\Delta_{\text{max}}$  may be interpreted as the coherence length of a virtual source with spectral a width of  $\Delta\nu$ [10,16]. In order to image static and moving constituents in a turbid sample at depths to  $\Delta_{\text{max}}=2$  mm, a spectral resolution of  $\Delta\nu=27$  GHz ( $\Delta\lambda=0.06$  nm) is required. Detection of  $P_{\text{ODT}}(\nu, t)$  over the power spectral density of the proposed high power low coherence source (i.e., 50 nm) requires a linear detector array with 1024 pixels. Measurement of the Doppler frequency shift ( $\Delta f_D$ ) of blood flow with a velocity of 1-4 mm/sec and  $\theta=70^\circ$ , requires a 10 kHz linear array frame rate.

To record spectral interference fringe intensity in the spatially-filtered optical spectrum analyzer, we propose to use a high-speed digital CCD linear detector array (1024  $\times$  256 pixels) designed for spectroscopic studies of chemical reactions (Fig. 4). In the operation of the linear array, a solitary row (1024 pixels) of photodetectors is active while remaining rows are masked for image storage and transfer. Low noise, high speed linear frame rates are achieved by shifting acquired spectra to successive masked rows. Up to 250 spectra may be acquired in a single burst at rates up to 300 kHz. Using the high speed CCD linear detector array in burst mode, lateral scans are performed by recording 250 spectra (10 kHz) at each lateral position. These spectra are then read out with a high speed A/D converter, before moving to the next lateral position. Readout time for the full 250 spectra is 300 ms for a 1 MHz 16 bit A/D converter. Use of a 12-bit 25 MHz A/D converter allows an ODT velocity image (100 $\times$ 512 pixels) to be acquired in one second. The design of the spectrometer will be guided

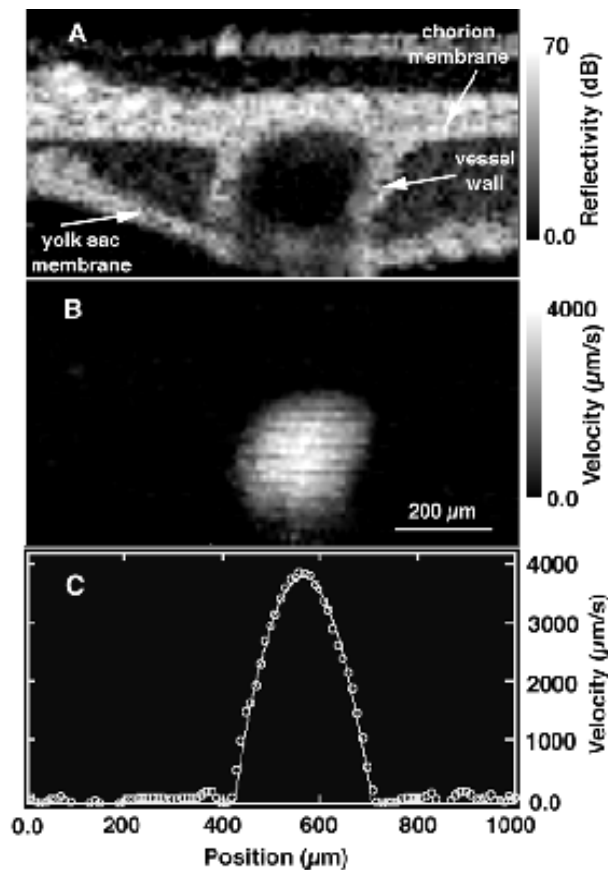


Figure 5. ODT images of in vivo blood flow in a CAM vein. A: ODT structural image, B: ODT velocity image, C: velocity profile along a horizontal cross section passing through the center of the vein, where the open circles are experimental data and the solid line is a parabolic fit.

by the spectral resolution (0.06 nm), full spectral range (50 nm), pixel size of the CCD array, and optimization of SNR.

#### System Integration, Testing and Optimization

Once the high power low coherence source, spectrometer, and CCD array are developed and individually tested, we will integrate these components with the fiber optic Michelson interferometer. Data acquisition and scanning control will be interfaced with a computer. Computational programs for ODT image construction from the time variation of spectral interference fringe data will be developed.

#### In vivo Chick Chorioallantoic Membrane (CAM)

To develop ODT for the clinical management of patients where blood flow monitoring is essential, feasibility studies must be conducted in biological models. The CAM is an established biological model for studying microcirculation and has been investigated extensively in our laboratory [12-13]. Because the CAM microvasculature is located in a transparent matrix, direct viewing of the blood vessels throughout their course is possible [21-22]. Once the apex of the chick eggshell is removed by opening a 2 cm diameter round window. The extensive three-dimensional nature of the CAM vascular network allows to be selected a wide range of horizontal/vertical individual blood vessel orientations and, therefore, Doppler shifts. To be selected CAM vessels of different diameters, orientations, and types (vein/artery) will be imaged

using ODT. Effects of the pulsation of blood flow in arteries on the ODT image will be investigated. To demonstrate the potential applications of ODT for *in vivo* blood flow monitoring after pharmacological intervention, the effect of a vasoactive drug on the CAM vasculature was studied. Drops of the vasodilating drug, nitroglycerin, were applied topically to a CAM artery.

## Results

#### Signal to Noise Ratio Analysis

Although substantially reduced image acquisition times may be achieved by the parallel acquisition of spectral interference fringe intensity using an optical spectrum analyzer. Image quality may be degraded by the loss of the signal to noise ratio ( $SNR_{ODT}(v)$ ).  $SNR_{ODT}(v)$  can be calculated by considering light in a narrow bandwidth ( $\Delta v$ ) centered at optical frequency  $v$ , detected by a single element of the linear array of the optical spectrum analyzer [23]. Noise in the measured spectral interference fringe intensity is due to three sources: (1) read noise ( $\delta N_m^2$ ) of each detector element in the linear array; (2) shot noise ( $\delta N_{sn}^2$ ) due to the discrete nature of the photodetection process (i.e., an absorbed photon creates a free electron and hole); and (3) photon bunching noise ( $\delta N_{pb}^2$ ) of light confined to a narrow spectral bandwidth ( $\Delta v$ ):

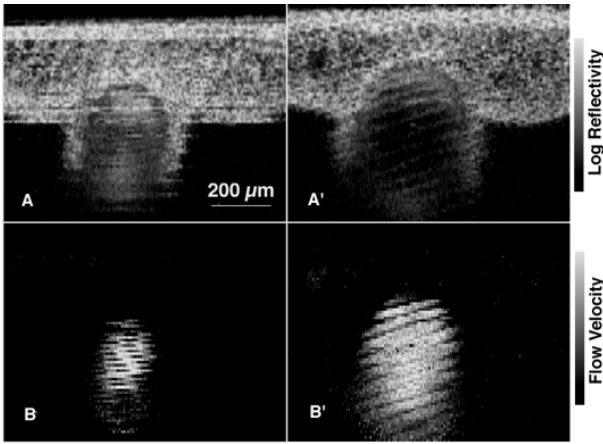


Figure 6. Effect of the vasodilating drug nitroglycerin on blood flow in a CAM artery. ODT structural and velocity images before (A, B) and after the application of topical nitroglycerin (A', B').

$$\delta N_m^2 = \frac{4K_B TC_{\text{eff}}}{e^2}; \quad (3)$$

$$\delta N_{\text{sn}}^2 = \frac{2P_r(\nu)\Delta t_p}{h\nu n_{\text{smp1}}} = 2N_r; \quad (4)$$

$$\delta N_{\text{pb}}^2 = \frac{2\Delta t_p P_r^2(\nu)}{\Delta\nu(h\nu)^2} = \frac{2n_{\text{smp1}} N_r^2}{\Delta t_p \Delta\nu}; \quad (5)$$

We use expressions for the number of detected photons in reference ( $N_r$ ) and sample ( $N_s$ ) paths. Additionally, we have assumed reference power ( $P_r(\nu)$ ) at the interferometer output.

This is much larger than that backscattered from the sample ( $P_s(\nu)$ ). So that shot and photon bunching noises are due to fluctuations in the reference power. Given these assumptions,  $\text{SNR}_{\text{ODT}}(\nu)$  [dB] is,

$$\text{SNR}_{\text{ODT}}(\nu) = 10 \log \left[ N_s(\nu) \left( \frac{2k_B TC_{\text{eff}}}{N_r(\nu)e^2} + 1 + \frac{n_{\text{smp1}} N_r(\nu)}{\Delta t_p \Delta\nu} \right) \right] \quad (6)$$

where we have assumed,  $P_{\text{ODT}}^2(\nu) = P_s(\nu)P_r(\nu)$ ;  $n_{\text{smp1}}$  is the number of times  $P_{\text{ODT}}(\nu)$  is sampled by the linear detector array within a pixel acquisition time ( $\Delta t_p$ );  $k_B$  is Boltzman's constant;  $T$  is the temperature of the linear detector array in the optical spectrum analyzer;  $C_{\text{eff}}$  is the effective capacity of a single detector element in the linear array; and  $e$  is the elementary charge.

#### ODT Images of *in vivo* Blood Flow in CAM

The CAM is a well established model for studying the microvasculature and the effects of vasoactive drugs on blood vessels [13]. Because the CAM microvasculature is located in a transparent matrix, direct viewing and noninvasive imaging of the blood vessels is possible after the apex of the chick eggshell is removed. The blood vessel wall, chorion membrane, and yolk sac membrane are evident in the ODT structural image (Fig. 5-A). In the ODT velocity image (Fig.

5-B), static regions ( $v=0$ ) in the CAM appear dark, while blood flowing at different velocities is evident. Since no blood flow pulsation is observed in the ODT velocity image, we conclude that the imaged vessel is a vein. Magnitude of blood flow velocity at the vessel center is maximal and decreases monotonically towards the lumen wall. Because a parabolic function provides an excellent fit to the velocity profile, along a horizontal cross section passing through the center of the vein (Fig. 5-C), we conclude that blood flow in the CAM vein is laminar. Diameters of the vein and artery are approximately 200 and 350  $\mu\text{m}$ , respectively.

ODT images before (Fig. 6-A, B) and after (Fig. 6-A', B') nitroglycerin application were obtained. The arterial wall is easily identified and dilation of the vessel after nitroglycerin application is evident in the ODT structural images. Increased cross sectional area and volumetric blood flow rate are observed in the ODT velocity images. Linear striations in ODT velocity images of arterial flow (Fig. 6-B and B') have an aliasing effect on blood flow pulsation and lateral scan frequencies. The arterial wall can be clearly identified and dilatation of the vessel after nitroglycerin application is observed in the structural images. Although velocity images appear discontinuous due to arterial pulsation, enlargement of the cross sectional area of blood flow is evident. Peak blood flow velocity at the center of the vessel increased from 3000 to 4000 m/s after nitroglycerin application. Dilatation of the vein due to nitroglycerin is observed in both structural and velocity images. In contrast to the artery, the peak velocity at the center of the vein decreased from 2000 to 1000  $\mu\text{m/s}$  after nitroglycerin application.

#### Discussion

The exceptional high spatial resolution of ODT has broad implications for the clinical management of patients where blood flow monitoring is essential. Information provided by ODT could be used, for example, to monitor perfusion and viability before, during, and after reconstructive procedures; to determine the efficacy of pharmacological intervention for failing surgical skin flaps or replants; to image micro-circulation during sepsis; and to evaluate tissue necrosis. ODT could also be applied to various nonmedical applications where rapid noninvasive imaging of turbulent or laminar flow is required. Given the noninvasive nature of the measurement, exceptional spatial resolution, simple hardware requirements, and relatively compact size, ODT is a promising technique for both basic research and clinical medicine.

High spatial resolution noninvasive techniques for *in vivo* blood flow imaging are currently not available as a diagnostic tool in clinical medicine. Such techniques could have a significant impact for biomedical research and clinical diagnosis [1,3-4]. The rationale for using ODT to characterize the underlying microvasculature is that the technique will be able to probe user-specified locations with high spatial resolution (2-15  $\mu\text{m}$ ) in light scattering biological tissues. Such localization is possible because the detected ODT interference fringe intensity gives an accurate discrimination

of the optical path length of Doppler shifted and backscattered light to within the source coherence length. Furthermore, in contrast to conventional LDF, the overall ODT signal from moving RBC is almost entirely due to the Doppler shifted light. As a result, signal-to-noise ratios (SNR) are substantially higher.

The importance of noninvasive imaging of the microvasculature in reconstructive surgery is underscored by the reported high salvage rates of failing flaps and replants (60-80%). Important diagnostic procedures expected to evolve from ODT are: (1) Determining tissue perfusion and viability before, during, and after surgical reconstructive procedures. (2) Assessing the efficacy of pharmacological intervention for failing surgical flaps or replants. (3) Evaluating the skin microcirculation for a variety of lesions before, during and after treatment. (4) Monitoring intraocular blood flow. In our high resolution ODT instrumentation, light backscattered from the turbid sample is coupled back into the fiber and forms interference fringes at the photodetector. Temporal interference fringe intensity ( $\Gamma_{ODT}(\tau)$ ) is measured by a single element silicon photovoltaic detector. Where  $\tau$  is the time delay between light from the reference and sample arms, and is related to the optical path length difference ( $\Delta$ ) between the two by  $\tau=\Delta/c$ , and  $c$  is the speed of light. High axial spatial resolution is possible because interference is observed only when  $\tau$  is within the source coherence time  $\tau_c$ , or equivalently, when  $\Delta$  is within the source coherence length ( $L_c=\tau_c c$ ). The interference fringe signal is amplified, band passed, digitized (20 kHz) with a 16-bit analog-to-digital (A/D) converter, and transferred to a computer workstation for data processing.

Power spectrum of the temporal interference fringe at the  $i$ th pixel is calculated by a fast Fourier transform (FFT):

$$\Gamma_{ODT}(\tau_i, f_m) = |FET(f_m; \Gamma_{ODT}(\tau_i, t))|^2 \quad (7)$$

where  $f_m$  is the discrete frequency value. A tomographic structural image is obtained by calculating the value of the power spectrum at the phase modulation frequency ( $f_0$ ). Because the magnitude of the temporal interference fringe intensity decreases exponentially as depth in the turbid sample increases, a logarithmic scale is used to display the ODT structural images:

$$S_{ODT}(i) = 10 \cdot \log(\Gamma_{ODT}(\tau_i, f_0)) \quad (8)$$

Fluid flow velocity at the pixel is calculated by the Doppler frequency shift ( $\Delta f_D$ ), which is determined by the difference between the carrier frequency, established by the optical phase modulation ( $f_0$ ) and the centroid ( $f_c$ ) of the measured power spectrum at the pixel:

$$v_{ODT}(i) = \frac{\lambda_0 \Delta f_D}{2ncos(\theta)} = \frac{\lambda_0 (f_c - f_0)}{2ncos(\theta)} \quad (9)$$

ODT measures the amplitude and frequency of the interference fringe intensity generated between reference and target arms of a Michelson interferometer to measure structure and velocity in images. High spatial resolution is possible because light

backscattered from the sample recombines with the reference beam and forms interference fringes only when the optical path length difference is within the coherence length of the source light. When light backscattered from a moving constituent interferes with the reference beam, beating at the Doppler frequency occurs ( $\Delta f_D$ ):

$$\Delta f_D = \frac{1}{2\pi} (\mathbf{K}_s - \mathbf{K}_i) \cdot \mathbf{v} \quad (10)$$

Where,  $\mathbf{k}_i$  and  $\mathbf{k}_s$  are wave vectors of incoming and scattered light respectively, and  $\mathbf{v}$  is the velocity vector of moving particles. With knowledge of the angle between the scattering vectors ( $\mathbf{k}_s - \mathbf{k}_i$ ) and the velocity ( $\mathbf{v}$ ), measurement of the Doppler frequency shift ( $\Delta f_D$ ) allows determination of particle velocity at discrete user-specified locations in a turbid sample. We have assumed,  $\mathbf{k}_s = -\mathbf{k}_i$  and  $\theta$  is the angle between  $\mathbf{k}_i$  and  $\mathbf{v}$ . The centroid of the measured power spectrum at the pixel is given by:

$$F_c = \sum_m f_m \Gamma_{ODT}(\tau_i, f_m) / \sum_m \Gamma_{ODT}(\tau_i, f_m) \quad (11)$$

Lateral and axial spatial resolutions of our prototype ODT instrument are limited by the beam spot size and source coherence length ( $L_c$ ) to 5 and 13  $\mu$ m, respectively. Higher axial resolution may be achieved by using a low coherence source with greater bandwidth. Velocity resolution in our prototype instrument (100  $\mu$ m/s) is dependent on the pixel acquisition time ( $\Delta t_p$ ) and the angle ( $\theta$ ) between flow velocity ( $\mathbf{v}$ ) and the incoming light direction ( $\mathbf{k}_i$ ) in the turbid sample. Velocity resolution may be improved with a smaller angle ( $\theta$ ) or longer pixel acquisition time ( $\Delta t_p$ ). Using our prototype instrument, the approximate time to record simultaneously ODT structural and velocity images is 3 minutes (e.g., 1 $\times$ 1 mm<sup>2</sup>, 5 $\times$ 13  $\mu$ m<sup>2</sup> resolution).

The effect of pharmacological intervention using nitroglycerin on the CAM vein and artery has been observed in our *in vivo* study. Nitroglycerin is a vasodilator used in the treatment of ischemic and congestive heart disease. The vasoactivity of nitroglycerin, as well as other nitrate compounds, arises from vascular metabolism to nitric oxide (NO) [24]. Although the conversion of nitroglycerin to NO remains incompletely understood, a membrane bound enzyme that involves sulfhydryl groups has been suggested [24]. Once generated, NO activates soluble guanylate cyclase, which makes a second messenger cGMP within the vascular smooth muscle cell. This, in turn, suppresses intracellular calcium, which leads to vascular smooth muscle relaxation [25]. It has also been observed that nitrovasodilators are venoselective irrespective of their mechanism of transformation. This suggests that NO itself may be venoselective *in vivo*. The peak blood flow velocity at the center of the artery is larger than the vein after the application of nitroglycerin. This is probably due to the reversal of oxygenation in CAM vasculature, where arteries and veins are oxygen poor and rich, respectively, because the embryo oxygenates itself from the surrounding air through the shell [13]. In humans, *in vivo*

vessels clearly show that NO is ten times more potent in veins than in arteries. Whereas *in vitro* vessels show much less selectivity [26]. The reason for this difference is unclear but it may involve other substances or cells found in human blood. The reversal of oxygenation could result in a reversal of selectivity, making nitroglycerin arterioselective in the CAM. However, determining the mechanism of vasoselectivity in CAM requires further investigations. Our results demonstrate that ODT offers a noninvasive method to image *in vivo* blood flow dynamics and surrounding tissue structure. The exceptionally high spatial resolution of ODT has broad implications for the clinical management of patients where micro-vascular blood flow monitoring is essential. Information provided by ODT can be used to determine tissue perfusion and viability before, during, and after surgical reconstructive procedures. It can also be used to assess the efficacy of pharmacological intervention for failing surgical flaps or replants; evaluate the skin microcirculation in a variety of lesions before, during and after treatment; and investigate the mechanism of Photodynamic Therapy (PDT) for cancer treatment [27-34].

### Conclusions

We have developed an ODT system for noninvasive imaging of *in vivo* blood flow. Tomographic velocity images of *in vivo* blood flow in the CAM were obtained using ODT. Applications of this technique to monitor *in vivo* blood flow dynamics, changes in vessel structure in response to a vasoactive drug and are demonstrated. ODT is noninvasive and noncontact, possesses exceptional spatial resolution, and is a promising technique for both basic research and clinical medicine. Results of our work provide relevant optical, physical, and engineering data on ODT and characterization and monitoring of fluid flow. The research is expected to lead to the development of a new technology for the clinical management of patients where microvascular monitoring is essential. The broad, long term objective of the proposed research is to develop a noninvasive tomographic imaging technique, ODT, and to characterize and monitor blood flow with high spatial resolution (2-15  $\mu\text{m}$ ) at discrete user-specified locations in biological tissues with high light scattering properties.

### Acknowledgments

This project is supported by research grants awarded from the Biomedical Research Technology Program and the Institute of Arthritis and Musculoskeletal and Skin Diseases (1R29-AR41638-01A1 and 1R01-AR42437-01A1) at the National Institutes of health, the Whitaker Foundation (21025), and Dermatology Foundation. Support from the Department of Energy (DE-FG03-91ER61227) and the National Institutes of Health (RR-01192).

### References

- [1] E. Yamada, M. Matsumura, S. Kyo, and R. Omoto, "Usefulness of a prototype intravascular ultrasound imaging in evaluation of aortic dissection and comparison with angiographic study, transesophageal echocardiography, computed tomography, and magnetic resonance imaging", *Am. J. Cardiol.*, 75 : 161-165, 1995.
- [2] W.J. Manning, , W. Li, and R.R. Edelman, "A preliminary report comparing magnetic resonance coronary angiography with conventional angiography", *N. Engl. J. Med.*, 328: 828-832, 1993.
- [3] J.V. Chapman, "Blood flow measurements by Doppler ultrasound, in The Noninvasive Evaluation of Hemodynamics in Congenital Heart Disease, " J.V. Chapman and G.R. Sutherland, Editors. Kluwer: Dordrecht, The Netherlands, 57, 1990.
- [4] R.F. Bonner, and R. Nossal, "in Laser-Doppler Blood Flowmetry, " A.P. Shepherd and P.A. Oberg, Editors. Kluwer: Dordrecht, The Netherlands, 17, 1990.
- [5] Y. Yeh, and H.Z. Cummins, "Localized fluid flow measurements with an He-Ne laser spectrometer", *Appl. Phys. Lett.*, 4 : 176-178, 1964.
- [6] C.E. Riva, B. Ross, and G.B. Benedek, "Laser Doppler measurements of blood flow in capillary tubes and retinal arteries", *Invet. Ophthalmol.*, 11 : 936-944, 1972.
- [7] X.J. Wang, , T.E. Milner, Z. Chen, and J.S. Nelson, "Measurement of Fluid Flow Velocity Profile in Turbid Media using Optical Doppler Tomography", *App. Opts.*, 36 : 144-149, 1997.
- [8] Z. Chen, T.E. Milner, D. Dave, and J.S. Nelson, "Optical Doppler tomographic imaging of fluid flow velocity in highly scattering media", *Opt. Lett.*, 22 : 64-66, 1997.
- [9] D. Huang, et al., "Optical Coherence Tomography", *Science*, 254(5035) : 1178-1181, 1991.
- [10] A.F. Fercher, , "Optical coherence tomography", *J. of Biomedical Opt*, 1 : 157-173, 1996.
- [11] J.A. Izatt, , M.R. Hee, E.A. Swanson, C.P. Lin, D. Huang, J.S. Schuman, C.A. Puliافتو, and J.G. Fujimoto, "Micrometer-Scale Resolution Imaging Of The Anterior Eye In Vivo With Optical Coherence Tomography", *Archives Of Ophthalmology.*, 112(12) : 1584-1589, 1994.
- [12] Z. Chen, T.E. Milner, S. Srinivas, X.J. Wang, A. Malekafzali, M.J.C. van Gemert, and J.S. Nelson, "Noninvasive Imaging of *in vivo* blood flow velocity using optical Doppler tomography", *Opt. Lett.*, 22: 1119-1121, 1997.
- [13] S. Kimel, L.O. Svaasand, M. Hammer-Wilson, M.J. Schell, T.E. Milner, J.S. Nelson, and M.W. Berns, "Differential vascular response to laser photothermolysis", *J. Invest. Dermatol.*, 103 : 693-700, 1994.
- [14] A.F. Fercher, W. Drexler, C.K. Hizenberger, and G. Kamp, "Measurement of optical distance by optical spectrum modulation", *SPIE*, 2083(263), 1994.
- [15] A.F. Fercher, C.K. Kitzenberger, G. Kamp, and S.Y. El-Zaiat, "Measurement of intraocular distances by backscattering spectral interferometry", *Opt. Commun.*, 117 : 43-48, 1995.
- [16] M. Bail, J.M. Hermann, M.W. Lindner, and R. Ringler. "Optical coherence tomography with the "Spectral Radar"-Fast optical analysis in volume scatterers by short coherence interferometry in Bios Europ 96", Vienna, Austria: *SPIE.*, 1996.
- [17] M.D. Stern, , "Two-fiber laser Doppler velocimetry in blood: Monte Carlo simulation in three dimensions", *Appl. Opt.*, 32 : 468-476, 1993.
- [18] M.H. Koelink, F.F.M. de Mul, J. Greve, R. Graaff, A.C.M. Dassel, and J.G. Aarnoudse, "Laser Doppler blood flowmetry using two wavelengths: Monte Carlo simulations and measurements", *Appl. Opts.*, 33 : 3549-3558, 1994.



- [19] J.M. Schmitt, and K. Ben-Letaief, "Efficient Monte Carlo simulation of confocal microscopy in biological tissue", *J. Opt. Soc. Am. A.*, 13 : 952-961, 1996.
- [20] L. Goldberg, and D. Mehuys, "High power superluminescent diode source", *Electronics Lett*, 30: 1682-1684, 1994.
- [21] C.M. Hawkey, and T.B. Dennett, "Color atlas of comparative veterinary hematology: normal and abnormal blood cells in mammals, birds and reptiles", 1 st ed. Ames: Iowa State University Press, 1989.
- [22] T. Sawada, R.B. Rimler, and K.R. Rhoades, "Indirect hemagglutinin test that uses glutaraldehyde-fixed sheep erythrocytes sensitized with extract antigens for detection of Pasteurella antibody", *J. Clin. Microbiol.*, 15 : 752-756, 1982.
- [23] W.V. Sorin, and D.M. Baney, "A simple intensity noise reduction technique for optical low-coherence reflectometry", *IEEE Phot. Tech. Lett.*, 4 : 1404-1406, 1992.
- [24] J.A. Bauer, and H.L. Fund, "Arterial versus venous metabolism of nitroglycerin to nitric oxide: a possible explanation of organic nitrate venoselectivity", *J. Cardiovasc Pharmacol*, 28: 371-374, 1996.
- [25] E Bassenge, and J. Zanzinger, "Nitrates in different vascular beds, nitrate tolerance, and interactions with endothelial function", *Am. J. Cardiol.*, 70 : 23B-29B, 1992.
- [26] R.J. MacAllister, A.L. Calver, J. Reizbos, J. Collier, and P. Vallance, "Relative potency and arteriovenous selectivity of nitrovasodilators on human blood vessels: an insight into the targeting of nitric oxide delivery", *J. Pharmacol. Exp. Ther.*, 273 : 154-160, 1995.
- [27] CJ Chang, JY Yang, CJ Weng, FC Wei. "Pilot *in Vitro* Toxicity Study of 5-ALA and Photofrin® in Microvascular Endothelial Cells Cultures", *Journal of Clinical Laser Medicine & Surgery*, 15 : 83-87, 1997.
- [28] CJ Chang, YL Lai, CJ Weng. "Photodynamic Therapy of Facial Squamous Cell Carcinoma in Cats Using Photofrin®", *Chang Gung Medical Journal*, 21(1) : 13-19, 1998.
- [29] CJ Chang, CH Sun, LHL Liaw, JS Nelson, MW Berns. "In vitro and in vivo photosensitizing capabilities of 5-ALA compared to Photofrin® in vascular endothelial cells", *Lasers in Surgery and Medicine*, 24 : 178-186, 1999.
- [30] CJ Chang, JS Nelson. "Cryogen spray cooling and higher fluence pulsed dye laser treatment improve port wine stain clearance while minimizing epidermal damage", *Journal of Dermatology Surgery*, 25: 767-772, 1999.
- [31] CJ. Chang, SF Ma, and FC Wei. "In vitro and In vivo photosensitizing capabilities of 5-ALA in Vascular endothelial cells", *Chang Gung Medical Journal*, 22(2) : 181-188, 1999.
- [32] PS Huang, and CJ Chang. "Cryogen spray cooling in conjunction with pulse dye laser treatment of port wine stains of the head and neck", *Chang Gung Medical Journal.*, 24(8) : 469-475, 2001.
- [33] CJ Chang, SF Ma, FC Wei. "Photosensitizing capabilities of photofrin® in vascular endothelial cells", *Fotmosan J Surg.*, 34(6): 278-293, 2001.
- [34] CJ Chang, Kristen M Kelly, J Stuart Nelson. "Cryogen spray cooling and pulsed dye laser treatment of cutaneous hemangiomas", *Annals of Plastic Surgery.*, 46 : 577-583, 2001.
-